Journal of Catalysis **195,** 125–139 (2000)
doi:10.1006/jcat.2000.2986, available online at http://www.idealibrary.com on IDEAL®

Theoretical Models of Ethylene Polymerization over a Mononuclear Chromium(II)/Silica Site

Øystein Espelid and Knut J. Børve

Department of Chemistry, University of Bergen, Allégaten 41, N-5007 Bergen, Norway
E-mail: oystein.espelid@kj.uib.no; knut.borve@kj.uib.no

Received March 20, 2000; revised June 14, 2000; accepted June 19, 2000

Cluster models are constructed for mononuclear Cr(II) sites of the Cr/SiO_2 Phillips catalyst for ethylene polymerization, displaying chromium covalently bound to two oxygen ligands. Based on these models, gradient-corrected density functional theory has been used to compare different routes of initiation and chain propagation with respect to structure, thermodynamical, and kinetical properties. It is shown that, for these sites, propagation mechanisms that involve four-coordinated chromium lead to activation energies that are incompatible with high catalytic activity. In the case of a chromacycloalkane intermediate, the relative rates of β-hydrogen transfer and monomer insertion are in agreement with the observed production of 1-hexene during early stages of polymerization. However, the anchoring site needs to be fairly strained before the activation energies drop significantly below 100 kJ/mol. On the other hand, a monoalkylchromium site supports insertion of ethylene into the Cr–alkyl bond according to the Cossee mechanism, with an activation energy of 56 kJ/mol relative to the ethylene–chromium precursor complex.

Key Words: **polymerization; ethylene; Phillips catalyst; density functional theory; initiation; propagation; cluster models.**

1. INTRODUCTION

The Phillips polymerization process (1) accounts for more than a third of the world production of polyethylene (2) and owes its popularity mainly to the broad range of polymers that may be produced (3). Phillips-type catalysts are composed of a chromium oxide impregnated on an amorphous support such as silica, e.g., Cr/SiO_2. They stand out among olefin polymerization catalysts by not requiring any cocatalyst and showing only low sensitivity to hydrogen in the feedstock (1). The polymers thus produced have notably broad molecular-weight distributions (1), and it would be of great interest to realize the strengths of Phillips catalysts within the concept of single-site catalysis (4). Such an endeavor would benefit from detailed insight in the reaction mechanisms and microscopic construction of the former (5), and an important step in this direction was the recent construction of a realistic working surface model (6). However, despite extensive research over many years, an understanding at the molecular level is still wanting for the Phillips catalysts (2). Nonetheless, the combined effort has provided invaluable information about the properties of the active sites, some of which will be reviewed next.

Following impregnation and calcination of the catalyst, chromium is left in a hexavalent state (1, 7) at a highly dehydroxylated silica surface (1). The monochromate-to-dichromate ratio has recently been shown to be dependent on the type of support and preparation procedure, and on industrial pyrogenic silica, monochromate species appear to be dominating at the surface (7). When the catalyst is brought into contact with ethylene, an induction time is observed prior to the onset of polymerization (1). This is attributed to a reduction phase, during which chromium is reduced to a divalent state and ethylene is oxidized to formaldehyde (8). The reduction may also be performed by means of carbon monoxide in a separate pretreatment step (9), in which case the induction period is replaced by a short delay consistent with initial adsorption of ethylene (1). In both cases, after reduction, chromium is found to have an average oxidation number just above 2 (1, 7–10), comprised of mainly Cr(II) and minute amounts of Cr(III) species. Based on FTIR spectroscopic studies of probe molecules, three families (A, B, C) of divalent chromium have been identified, where Cr is bonded to the surface through two ester linkages. They differ in the degree of coordinative unsaturation (A > B > C) (11–14) and, consequently, in their propensity to react. The Cr(II)-A sites are claimed to be the more active for polymerization (15, 14), although the activity may depend on the nuclearity of the Cr(II) site (16).

Phillips catalysts are unique in not requiring any alkylating agent to supply the starting polymer chain. It has been suggested that hydrogen supplied from surface silanol groups may serve this function (17, 18), but this is contrary to other claims that excellent catalysts may be obtained from a thoroughly dehydroxylated surface (1, 19). Hence, it appears that the starting structures evolve in a reaction between the reduced catalyst and ethylene. After coordination to the reduced chromium, ethylene has been suggested to rearrange to ethenylhydridochromium(IV) by means of hydrogen transfer to the metal (5, 20). Ethylene may then be inserted in either the chromium–hydride or the

0021-9517/00 $35.00

chromium–ethenyl bond. Alternatively, an ethylidene-chromium(IV) species may be formed through a metal-catalyzed transfer of hydrogen between the carbon atoms in ethylene (21). Recently, Amor Nait Ajjou *et al.* (22–24) prepared a working catalyst through thermal transformation of a dialkylchromium(IV) structure, accompanied by release of the corresponding alkane. The stoichiometry of this conversion is in accordance with a carbene starting structure. Chain growth from a carbene structure may conceivably take place via addition of ethylene to the chromium–carbon double bond, followed by α-hydrogen transfer to chromium and reductive elimination to restore the carbene functionality (21).

Several studies report the formation of 1-hexene in the early stages of polymerization (22, 25, 26). After the pre-reduced catalyst was exposed to C_2D_4, only fully deuterated 1-hexene mass fragments were observed (26), indicating activity without hydrogens from surface silanol groups. Selective trimerization of ethylene to form 1-hexene has been reported also for homogeneous chromium catalysts and proposed to proceed via metallacyclic intermediates (27). From this, chromacyclopentane, formed by coordinating two ethylene molecules to chromium, may also be considered a viable starting structure for polymerization. Further insertions may then take place to one of the two chromium–carbon single bonds.

The purpose of the present work is to make a quantitative comparison of the most topical of the initiation and propagation mechanisms suggested for the Phillips catalyst (1, 5, 20, 21, 24, 26). To this end, quantum chemical modeling is applied to cluster models of Cr(II)-A sites and used to derive structural and energetical information about the selected mechanisms. The feasibility of the various *initiation* mechanisms is discussed on the basis of thermodynamic stability of the intermediates postulated in each case. In the case of *propagation* mechanisms, the emphasis is placed on activation energies for monomer insertion into chromium–carbon bonds. This information is also used to address the more general question of whether the commonly held conception of the active site, as having the character of a chromate ester with two oxygen linkages to the silica surface, may be consistent with high activity toward polymerization. A preliminary account of this work was given at the WATOC'99 conference (28).

The main limitation in the present study is that it is confined to mononuclear Cr(II)-A sites. Some researchers suggest that the active sites may involve two chromium atoms, either in the form of neighboring monochromate groups (20, 29) or as dichromate species (30, 31). Furthermore, surface oxygens have been proposed to play a role in some mechanisms, either directly bonded to chromium (Si–O–Cr) (12), in siloxane bridges near a chromium center (Si–O–Si) (26), or in nearby surface silanol groups (Si–OH) (17, 18). In subsequent work, we aim to investigate also these proposals by means of quantum chemical modeling.

2. THE COMPUTATIONAL MODEL

2.1. The Quantum Chemical Method

This study was conducted using gradient-corrected density functional theory as implemented in the Amsterdam Density Functional (ADF) set of programs (32, 33). For the electron correlation part, the local potential by Vosko *et al.* (34) and the nonlocal correction by Perdew (35) (P86) were used. The exchange potential consists of the Slater functional augmented by gradient corrections as specified by Becke (36) (B). Closed- and open-shell systems were described within spin-restricted and -unrestricted formalisms, respectively.

Primitive STO basis sets supplied with ADF (32, 33) were used for all atoms. Atomic cores, defined as the K shell for first-row atoms and K and L shells for second- and third-row atoms, were described according to the frozen-core approximation. The number of basis functions used to describe each valence atomic orbital were as follows: H 1*s*, 2; C 2*s* and 2*p*, 2; O 2*s* and 2*p*, 3; Si 3*s* and 3*p*, 2; Cr 3*s* and 3*p*, 2; Cr 3*d* and 4*s*, 3; and Cr 4*p*, 1. A single set of *d*-type polarization functions were added to C, O, and Si, and a set of *p* functions were added to H. A set of auxilary atom-centered *s*, *p*, *d*, *f*, and *g* STO functions were used to afford an accurate fit of the electron density as well as Coulomb and exchange potentials.

Molecular geometries were converged to a gradient below 0.001 $E_H/Å$ and the accuracy of the numerical integration schemes adjusted accordingly. Transition-state searches were typically conducted in two steps; an initial linear-transit scan followed by transition-state optimization. The optimization was started at the top point of the linear-transit energy curve, with an analytical Hessian matrix computed in Gaussian94 (37) using 3-21G bases and the same functionals as defined above.

Extensive studies reported elsewhere (38) demonstrate that the B-P86 functional is capable of providing accurate energy profiles for the monomer insertion step during metal-catalyzed olefin polymerization. For later reference, the change in energy was computed for the organic reaction Ethylene + Ethane $\rightarrow$ *n*-Butane to be -98 kJ/mol.

2.2. Designing Cluster Models

Little is known about the surface morphology of the amorphous silica support used for commercial Phillips catalysts. On the other hand, silicalite, which is a structurally well-characterized siliceous zeolite, has been used successfully as support in experimental model studies (15, 29). It is found that medium-to-long polymer chains are produced at active sites at external surfaces of the thus prepared catalyst

(29). Moreover, since the calcination temperature is some 600 K below the degradation temperature of silicalite (39), it is likely that, apart from dehydroxylation, the more stable crystal faces, {010}, {100}, {001}, and {101}, undergo only moderate reorganization during calcination. Hence, these crystal faces may provide insight into the structure of topical sites for anchoring chromium to the support.

Following calcination of the catalyst, chromium is believed to be present as a chromate ester with two oxygen linkages to the silica surface, possibly formed through a condensation reaction between a chromium hydroxide and two surface silanol groups (1). Therefore, for the present purpose of constructing cluster models, an anchoring site is considered to consist of two surface hydroxyl groups close enough to facilitate bonding to the same chromium atom. These sites may be classified according to the number of silicon atoms encountered while traversing the shortest possible path through bonds connecting the two hydroxyl groups, n_{Si}. Geminal hydroxyl pairs ($n_{Si} = 1$) arise only at the {001} and {101} faces. In this case, the oxygen–oxygen distance between unrelaxed hydroxyls is approximately 2.6 Å. Hydroxyls connected by a single siloxane bridge ($n_{Si} = 2$) are present at all faces considered, with unrelaxed O–O distances ranging from 3.6 to 4.8 Å. Hydroxyls connected through two siloxane bridges ($n_{Si} = 3$) are also present at all surfaces, showing unrelaxed interhydroxyl distances between 3.9 and 6.0 Å. Hydroxyls connected through three or more siloxane bridges ($n_{Si} > 3$) only occasionally arise with O–O distances below 6 Å and are not considered further. Assuming equal areas of the most commonly exposed faces on the external surfaces, the density of anchoring sites is crudely estimated to 0.5, 1.5, and 2.5 sites/nm^2 for $n_{Si} = 1$, 2, and 3, respectively. The total density of surface hydroxyl may be estimated to 3.5–4.0 OH/nm^2, implying a saturation limit for monochromate species close to 2 Cr/nm^2.

To compare the stability of chromate esters attached to anchoring sites of different sizes, the sites were modelled by $H(OSiH_2)_{n_{Si}}OH$ oligomers. Starting from chromic acid, the anchoring reaction may proceed as suggested in Fig. 1, leaving chromium in its hexavalent state as part of a $(2 + 2n_{Si})$-membered ring.

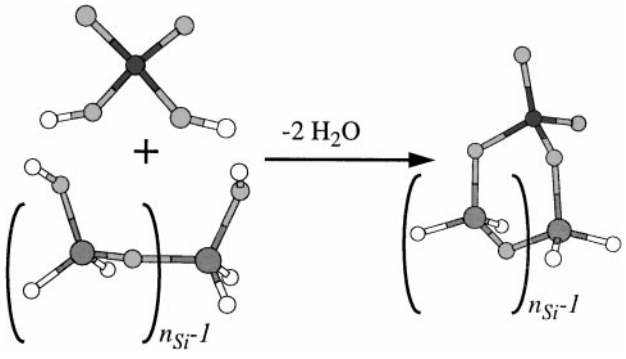

FIG. 1. Condensation reaction between chromic acid and a model anchoring site. The elements are coded on a gray scale according to H (white) < O < Si < Cr (dark gray).

Much due to reduced ring strain, the heat of the anchoring reaction was found to decrease with increasing ring size, from 103 kJ/mol for $n_{Si} = 1$ to 12 and −11 kJ/mol for $n_{Si} = 2$ and 3, respectively. In the two larger product clusters, the distances between the oxygen atoms bridging to chromium are 2.81 and 2.88 Å, respectively, quite similar to the interhydroxyl distance in chromic acid of 2.93 Å. Furthermore, these optimized distances are notably shorter than O–O distances at anchoring sites characterized by $n_{Si} = 2$ and 3 at silicalite. This implies that the anchoring reaction leads to substantial surface relaxation, in particular, for the $n_{Si} = 3$ case. Thus, it appears likely that chromate esters may be formed preferentially at $n_{Si} = 2$ sites and only the more flexible of the $n_{Si} = 3$ sites.

The silicachromates appearing as products in Fig. 1 will be used as cluster models of chromates formed at different surface sites. As such, each cluster may be thought of as cut from a surface, followed by saturation of two dangling bonds at each silicon atom by means of hydrogen. Such a model ignores long-range electrostatic interactions and lacks the strain from the rest of the surface, but it may be expected to describe local electronic effects quite well (40).

It is of interest to compare the cluster models with respect to geometry parameters, cf. Table 1. The most pronounced difference is found for the ∠OCrO angle, which in the case of the reduced clusters, increases from 86° (for $n_{Si} = 1$), via 116°, to 135° in the $n_{Si} = 3$ cluster. Apart from this, bond lengths and angles differ by less than 0.01 Å and a few degrees between the two larger clusters considered, compared to slightly longer Cr–O bonds in the $n_{Si} = 1$ cluster. Table 1 also contains data for chromic acid and chromium dihydroxide, which resemble the chromate and reduced clusters in the local structure about chromium. The main point to note here is that ∠OCrO is significantly more open in the dihydroxide than it is in any of the cluster models. Thus, even though the $n_{Si} = 3$ cluster is flexible, at least in the reduced state it does offer some constraints on the configuration about chromium. In the $n_{Si} = 2$ cluster, ∠OCrO is about 30° narrower than that in the dihydroxide, demonstrating that the six-membered ring is quite strained.

Feher and Blanski prepared the chromate ester of a silasesquioxane cage compound terminated by cyclohexyl groups (41). This molecule may be viewed as a structural model of the oxidized Phillips catalyst, even though it does require a cocatalyst before even moderate activity with respect to polymerization is obtained. Apart from the size of this molecule, it constitutes an interesting model also for computational studies. Hence, the present quantum chemical methods were applied to determine the geometry of a modification of this molecule in which silicon was saturated by hydrogen atoms rather than cyclohexyl

TABLE 1

Geometry Parameters of Chromic Acid, Chromate Ester Clusters, the Chromate Ester of a Silasesquioxane (1), and the Corresponding Reduced Structures

		Cyclic chromate clusters			
	$O_2Cr(OH)_2$	$n_{Si}=1$	$n_{Si}=2$	$n_{Si}=3$	**1** (exp.)[a]
*r*Cr–O	1.78	1.79	1.77	1.77	1.76 (1.73)
*r*Cr=O	1.59	1.59, 1.59	1.59, 1.60	1.59, 1.59	1.59 (1.56, 1.57)
∠O–Cr–O	111	88	105	109	109 (109.5)
∠O–Cr=O	107, 110	114, 115	109, 112	109,110	109, 110 (108-110)
∠O=Cr=O	112	110	110	110	110 (109)
		Reduced clusters			
	$Cr(OH)_2$	$n_{Si}=1$	$n_{Si}=2$	$n_{Si}=3$	Reduced **1**
*r*Cr–O	1.82	1.85	1.82	1.82	1.82
∠O–Cr–O	146	86	116	135	134

Note. Units: bond lengths (*r*) in Å; angles (∠) in degrees.

[a] Experimental values within parentheses from Ref. (41). Additional parameters, calc. (exp.): ∠CrOSi = 131° (135°) and ∠SiOSi = 141°–147° (145°–149°).

moieties; see Fig. 2 Selected parameters for the optimized geometry may be found in Table 1, together with structural data obtained from single-crystal X-ray diffraction. As is apparent from Table 1, the ∠OCrO bond angles are predicted in good agreement with experiment. The chromium–oxygen bonds are computed a few pm too long and the bond angles of the framework oxygens turn out somewhat pointed. Similar deviations were also found when comparing geometry parameters for a series of chromium oxides and oxohydroxides with those obtained in more accurate calculations (42).

Further comparisons may be made to experimental data obtained by Raman spectroscopy for a dehydrated, silica-supported chromium oxide catalyst. Based on an empirical frequency-bond length correlation, the *r*Cr=O bond lengths were estimated to 1.57 ± 0.03 Å (43). The present computational model leads to an average *r*Cr=O bond length of 1.59 Å (see Table 1) for our cluster models of oxidized chromium on silica supports. Thus, our computed chromium–oxygen bond distances appear to be systematically long, by a couple of pm. This should, however, not be taken as an indication of underestimated metal–ligand interactions. Harmonic Cr=O stretching frequencies are computed at 1016 and 1054 cm^{-1} for the $n_{Si}=2$ silicachromate cluster, compared to experimental fundamental frequencies of 986 ± 46 cm^{-1} for a dehydrated silica-supported chromium oxide catalyst (43). The agreement is expected to improve further upon correcting for anharmonicity effects.

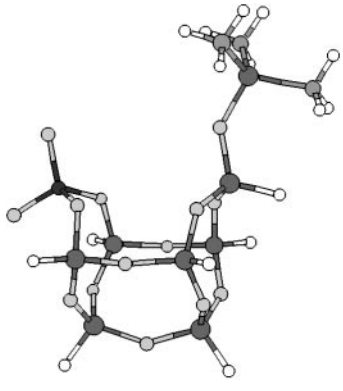

FIG. 2. The chromate ester silasesquioxane of Ref. [41], terminated by hydrogen instead of cyclohexyl groups. The elements are coded on a gray scale according to H (white) < O < Si < Cr (dark gray).

It is also of interest to compare computed and observed energies of *d–d* transitions for a reduced Cr/SiO_2 catalyst. Using the $n_{Si=2}$ cluster as a model, we compute the first *d–d* transition, $^5A'–^5A''$, at a vertical transition energy of 10,400 cm^{-1}. This agrees very well with the observed band maximum at 10,000 cm^{-1}, ascribed to *d–d* transitions in Cr^{2+} ions at sites of lower-than-octahedral symmetry (44).

The present level of theory appears to reproduce the main qualities of the geometric and electronic structure of Cr bonded through two covalent bonds to the silica surface. Apart from the narrower ∠OCrO angle in the six-membered ring, the local structure about chromium is computed very similarly for the $n_{Si}=2$ and $n_{Si}=3$ clusters as well as for the Feher–Blanski model. At the surface, restoring forces are likely to limit the flexibility of this parameter. Hence, the $n_{Si}=2$ cluster is chosen as our main model on account of it being a reasonable model of silica-anchored chromium as well as amenable to calculations. The $n_{Si}=1$ and $n_{Si}=3$ clusters will be used to examine how reactivity depends on ∠OCrO.

3. RESULTS

3.1. Coordination of Ethylene

The $n_{Si} = 2$ chromate cluster adopts a tetrahedral arrangement about chromium. The reduced cluster retains C_s symmetry (see Fig. 3) and the $^5A''$ ground state contains four unpaired *d* electrons. The net charge on chromium is 1.0*e* in the reduced cluster model, compared to 1.7*e* in the corresponding chromate cluster. Ethylene may coordinate in two different ways to the reduced cluster, either as a molecular complex or covalently bound to chromium, cf. Table 2 for structural parameters.

At chromium–carbon distances of 2.36 and 2.38 Å, an ethylene–chromium π complex forms in which the four *d* electrons on chromium remain high-spin coupled. Only minor changes take place in Mulliken populations and the geometry of either ethylene or the cluster, indicating that the charge transfer is very modest. A likely explanation is that repulsion to Cr 3*d* prevents the formation of an efficient donation bond. The binding energy is accordingly a mere 68 kJ/mol.

At a shorter chromium–carbon distance of about 2.02 Å, a triplet-coupled complex is formed, cf. **3a** in Fig. 4. In this complex, improved donation to the metal as well as back-donation to ethylene act to compensate for the loss in 3*d* exchange energy. The binding energy remains low, at 69 kJ/mol, but the net charge on chromium increases to 1.4*e*, and ethylene acquires a charge of −0.4*e*. The carbon–carbon bond lengthens to 1.45 Å, compared to 1.36 Å in the molecular complex (see Table 2). It is interesting to compare the structure of this covalently bound complex to that of an ethylene–Cr(III) complex reported by Emrich *et al.* (27). They found a C−C bond length of 1.415 Å and Cr−C distances of 2.008 Å. Considering that the higher oxidation state probably leads to less repulsion between the olefin and the metal, but also less back-donation, the agreement with our data is considered good.

The two modes of ethylene coordination have been found also for the more flexible $n_{Si} = 3$ cluster. The structural parameters are similar to those discussed above, and the binding energies are computed at 51 and 72 kJ/mol for the molecular and covalently bound complexes, respectively. Thus, it appears that the latter binding mode dominates when the coordination site has more flexibility, and the studies of initiation mechanisms are based on an initial coordination of ethylene in the covalent mode.

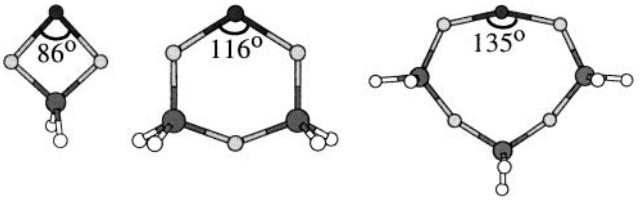

FIG. 3. Reduced cluster models: $n_{Si} = 1$ (left), $n_{Si} = 2$ (middle), and $n_{Si} = 3$ (right). The elements are coded on a gray scale according to H (white) < O < Si < Cr (dark gray).

TABLE 2

Geometry Parameters for Ethylene Coordination to the Reduced $n_{Si} = 2$ Cluster

	Molecular complex	Covalently bound
$r\mathrm{CrC}_1$	2.36	2.02
$r\mathrm{CrC}_2$	2.38	2.03
$r\mathrm{C}_1\mathrm{C}_2$	1.36	1.45
$r\mathrm{CrO}$	1.83–1.86	1.78
∠OCrO	107	113

Note. Units: bond lengths (*r*) in Å; angles (∠) in degrees.

3.2. Initiation Phase

The polymerization reaction may formally be divided into three phases, denoted by initiation, propagation, and termination, respectively. The present section is devoted to the initiation phase and serves a two-fold purpose. First, it is of interest to examine how the different routes of chain propagation may be entered, starting from a reduced catalyst and ethylene. Second, by deriving stability data for intermediates occurring in the various initiation schemes, one may facilitate a quantitative comparison of these mechanisms. A single-cluster model is used throughout, implying that rearrangement of the substrate is not taken into account.

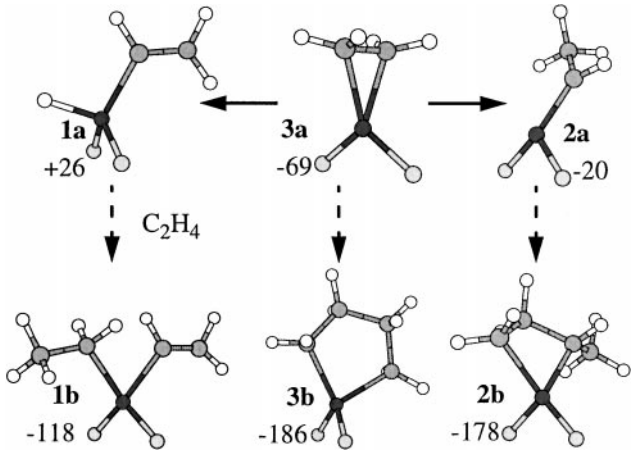

FIG. 4. Relationship between different proposals with respect to the initiation phase. **3a**, ethylene–Cr π-complex (^{3}A); **1a**, ethenylhydridochromium; **2a**, ethylidenechromium; **3b**, chromacyclopentane; **1b**, ethenylethylchromium; **2b**, chromacyclo(methyl-)butanechromium. The elements are coded on a gray scale according to H (white) < O < C < Cr (dark gray), and only the oxygen atoms bridging to Cr are shown from the silica cluster. Energies (kJ/mol) are given relative to free monomers and the reduced cluster.

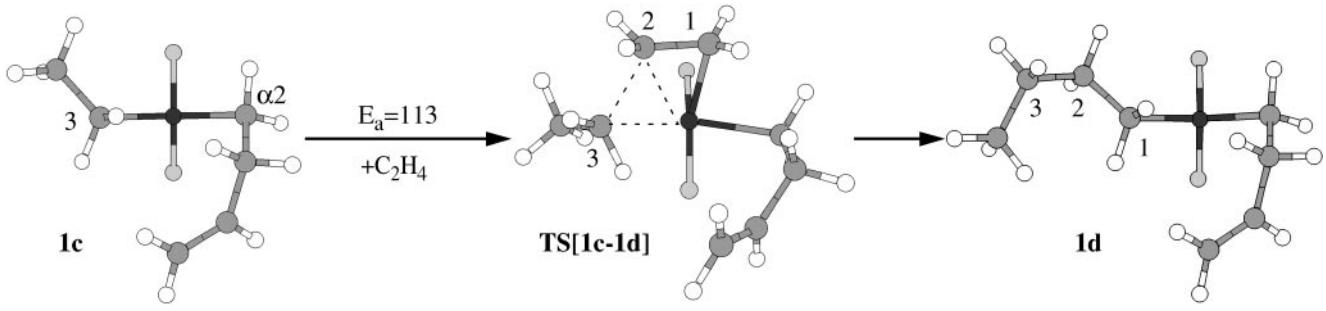

FIG. 5. Stationary points along the reaction path of ethylene insertion into the Cr–ethyl of a but-3-enylethylchromium species (**1c**) with transition state (**TS[1c-1d]**), and product but-3-enylchromium (**1d**). The elements are coded on a gray scale according to H (white) < O < C < Cr (dark gray), and only the oxygen atoms bridging to Cr are shown from the silica cluster. Activation energies in kJ/mol.

3.2.1. Ethenylhydridochromium(IV). Ethylene may react with the reduced catalyst in an oxidative addition reaction (5, 20), resulting in the ethenylhydrido species included as **1a** in Fig. 4. Chromium is left in oxidation state IV, and the overall reaction to reach the $^3A''$ ground state is endothermic by 26 kJ/mol relative to free reactants. Subsequent insertion of ethylene into the chromium–hydride bond gives rise to an ethenylethylchromium species, structure **1b** in Fig. 4, a reaction that is exothermic by 144 kJ/mol. Despite a rather short Cr–ethenyl bond of 1.98 Å, this bond is actually weaker than the Cr–ethyl bond, and a second insertion presumably takes place to the former. The chromium–carbon bonds in the thus formed but-3-enylethylchromium species (**1c**, Fig. 5), have single-bond characters, with lengths of 2.00 Å. Moreover, there is no tendency for the alkenyl to act as a bidentate ligand. Insertion into either of the Cr−C bonds is therefore expected to follow the pattern of a dialkylchromium with respect to chain propagation.

3.2.2. Ethylidenechromium(IV). Another conceivable mode of initialization is the formation of an ethylidenechromium species (21) (see **2a** in Fig. 4), by means of hydrogen transfer from one end to the other of an ethylene molecule coordinated to the reduced catalyst. In **2a**, the ligands are arranged in a close-to-planar configuration about chromium. The double-bond character in the Cr−C bond is significant, decreasing the bond length to 1.82 Å. Still, the overall reaction is exothermic by a mere 20 kJ/mol relative to free reactants.

3.2.3. Methylidenechromium(IV) from Dimethylchromium(IV). Rather than generating an initial carbenechromium structure by rearrangement of ethylene, one may start out from a dialkylchromium intermediate. Intramolecular α-H elimination is considered for a dimethylchromium(IV) complex, to give methane and methylidenechromium as products. This reaction may proceed either according to a concerted one-step mechanism or by formation of a hydrido intermediate. For the present system, the formation of a hydridomethylmethylidene–Cr(VI) intermediate is endothermic by 245 kJ/mol and thus prohibitively costly. The concerted reaction path is also energy demanding and requires an activation energy of 164 kJ/mol. In the transition state, the transferring hydrogen lies in the plane defined by O−Cr−O, at a distance of 1.72 Å from chromium. The transition state is located late along the reaction path as evidenced by bond lengths of 1.84 Å for the forming chromium–carbene bond and 1.55 and 1.44 Å for the breaking and forming C−H bonds, respectively. The second Cr−C bond, eventually to be broken in the product, is stretched to 2.21 Å, and the ∠CCrC bond angle is narrowed by 15° to 92°. The methylidenechromium product adopts C_s symmetry in its $^3A''$ ground state, featuring a short Cr=C distance of 1.82 Å. The overall reaction to form the chromium carbene species is endothermic, by 107 kJ/mol.

3.2.4. Chroma(IV)cyclopentane. Starting from a single ethylene covalently bound to the reduced $n_{Si}=2$ cluster (**3a** in Fig. 4), a second monomer may coordinate with an energy of −50 kJ/mol to give a double π-complex, **3π**, in Fig. 7. A chromacyclopentane structure may subsequently form by fusing a carbon–carbon bond between the two ethylene units. The transition state, (see **TS[3π-3b]** in Fig. 7) is positioned at a forming C−C bond distance of 2.08 Å. The corresponding energy barrier is only 9 kJ/mol, and the overall reaction energy from **3a** and ethylene to the chromacyclopentane product, **3b**, is −117 kJ/mol.

Two conformations are found for **3b**, analogous to the *twist* and *envelope* conformations of cyclopentane (45). In the twist conformation (**3b**), which is the lower by 12 kJ/mol, the carbon atoms have close to tetrahedral structure and all C−C bond lengths are about 1.53 Å. The angle ∠CCrC = 88° constitutes the main deviation from local tetrahedral geometry about the metal.

3.2.5. Rearrangement of chromacyclopentane. Other proposals with respect to starting structures involve intramolecular hydrogen transfer in the chromacyclopentane species. α-H transfer may occur between the two carbon atoms bonded to chromium, to produce a linear carbene species, butylidenechromium. Polymerization from such a starting structure is discussed as part of the carbene mechanism.

Another suggestion (1) involves hydrido(methyl-)allylchromium(IV), for which both triplet and quintet spin states have been examined with respect to thermochemical stability. In the triplet spin state, the methylallyl ligand may coordinate in two η^1 modes that differ with respect to which carbon atom is forming a covalent bond to chromium. In either case, the energy is up some 73 kJ/mol from that of the parenting chromacyclopentane structure. However, the single bond to chromium makes the allyl ligand take on the character of an alkenyl, and the energy drops nearly 30 kJ/mol if the double bond coordinates to chromium. The resulting structure shows an asymmetric η^3 coordination, with chromium–carbon distances of 2.07, 2.25, and 2.47 Å, and corresponding carbon–carbon bonds lengths of 1.43 and 1.38 Å, respectively. Following insertion of ethylene into the Cr–H bond to produce ethyl(methyl-)allylchromium, the allyl ligand reverts to a pure η^1 coordination mode.

In its quintet spin state, the hydridomethylallylchromium species features the allyl ligand bound in η^3 mode. However, this structure lies 154 kJ/mol above the parenting chromacyclopentane structure in energy.

3.3. Models of the Propagation Phase

3.3.1. A dialkylchromium(IV) site. Structure **1c** (but-3-enylethylchromium) (see Fig. 5) is considered as a starting structure for polymerization. The vinyl group in the but-3-enyl ligand opens for the possibility of a second coordination to the metal. However, such a coordination is not found, and **1c** appears to be functionally equivalent to a chromium dialkyl species as far as insertion of ethylene is concerned. Chromium's lack of affinity for the vinyl group is probably caused by repulsion between its nonbonding 3*d* electrons in the "t_2" orbitals and the π-electrons of the vinyl moiety. A similar mechanism prevents the formation of a proper coordination complex between the incoming monomer and **1c**. Chain growth must therefore proceed through direct insertion into either of the two chromium–carbon bonds, of which we have chosen to consider the chromium–ethyl bond. The transition state separating reactants from the but-3-enylbutylchromium product (**1d**), found at an energy of 113 kJ/mol above that of free reactants. The transition state itself has a distorted trigonal bipyramidal structure, with ethylene and an oxygen atom in axial positions, *c.f.* **TS[1c-1d]** in Fig. 5. The net charge of chromium is reduced by 0.21*e* to 1.27*e* relative to that of the starting but-3-enylethyl species, due to donation from the incoming ethylene. This leads to longer bonds between chromium and the remaining ligands, with changes between 4 and 8 pm. The ethylene double bond (C_1–C_2) is stretched to 1.43 Å, the forming Cr–C_1 bond is 2.15 Å, and the forming carbon–carbon bond (C_2–C_3) is 1.99 Å at the TS. The chromium–ethyl bond is stretched by approximataly 20 pm (see Table 3). The product **1d** resembles **1c** both with respect to local geometry about chromium and net charge and orbital occupation of the metal. The energy of the insertion reaction is −99 kJ/mol, i.e., very close to that of the organic reaction between ethane and ethene to give butane.

TABLE 3

Geometry Parameters for Stationary Points along the Reaction Path of Ethylene Insertion into the Cr–Ethyl Bond in a But-3-enylethylchromium Species (1c) with Transition State (TS[1c-1d]) and Product But-3-enylchromium (1d)

	1c	TS[1c-1d]	1d
rCrC$_1$	—	2.15	2.00
rCrC$_2$	—	2.39	2.99
rCrC$_3$	2.00	2.21	4.39
rC$_1$C$_2$	(1.33)[a]	1.43	1.52
rC$_2$C$_3$	—	1.99	1.54
rCrO	1.79	1.83–1.86	1.79
∠OCrO	111	99	111

Note. Units: bond lengths (r) in Å; angles (∠) in degrees.
[a] Free monomer.

Direct insertion of ethylene into a Cr–C bond is examined also for the case of an allyl(ethyl)chromium reactant. The allyl ligand adopts a η^1 coordination mode in the reactant, and the configuration about chromium is thus similar to that of a dialkylchromium species. However, at the transition state of ethylene insertion into the chromium–ethyl bond, an asymmetric η^3 coordination develops, characterized by chromium–carbon distances of 2.18, 2.31, and 2.56 Å, and carbon–carbon bonds lengths of 1.43 and 1.37 Å, respectively. This stabilizing interaction reduces the barrier to insertion by 32 kJ/mol relative to that of a standard dialkylchromium species, to 82 kJ/mol. The lengths of the forming carbon–carbon bond and the weakened ethylenic double bond are 2.06 and 1.42 Å, respectively, indicating an earlier transition state as compared to **TS[1c-1d]**.

3.3.2. A carbenechromium(IV) site. The first step of the carbene mechanism for polymerization is proposed to parallel the Chauvin mechanism (46, 47) for metathesis, i.e., $2_\pi + 2_\pi$ cycloaddition between an incoming ethylene and the carbene. Starting from chromium ethylidene, **2a**, the product is a chromacyclo(methyl-)butane species, included as structure **2b** in Fig. 6. The cycloaddition step was found to proceed without barrier and an energy of reaction of −158 kJ/mol. **2b** features two Cr–C single bonds as evident from bond lengths of 1.98–1.99 Å, compared to 1.82 Å in **2a**. The strain in the cyclobutane is considerable, with a ∠CCrC angle of 78° and ∠CrCC angles of approximately 82°. None of the α-H's of C_1 shows any specific interaction with Cr.

To arrive at a polymerization mechanism, it is necessary to regenerate the chromium carbene; i.e., **2b** needs to isomerize to butylidene chromium, shown as structure **2c** in Fig. 6. This requires intramolecular hydrogen transfer between the two α carbons in the chromacyclobutane moiety. In particular, to produce an unbranched polymer, the hydrogen must transfer from the α-carbon originating from

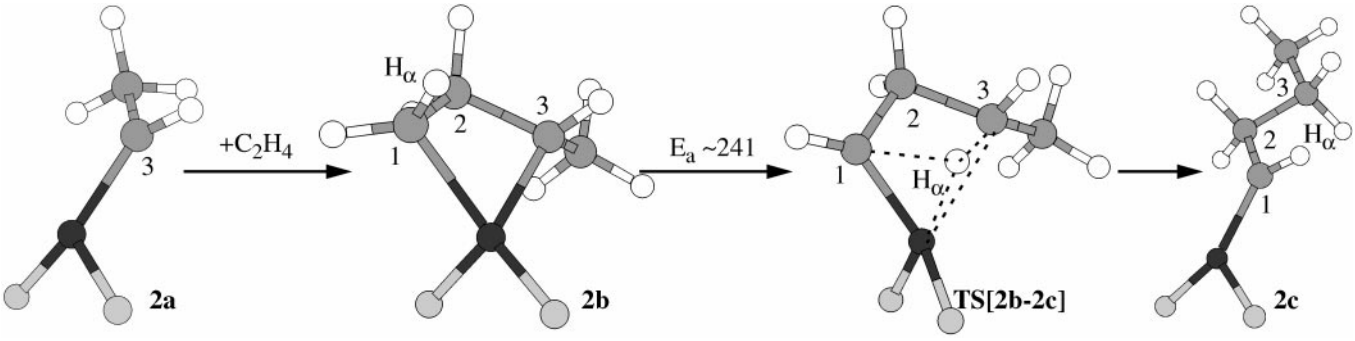

FIG. 6. Stationary points along the reaction path of ethylene insertion to an ethylidenechromium species **(2a)**, with cycloaddition product, chromacyclo(methyl-)butane (**2b**), the concerted α-H transfer transition state (**TS[2b-2c]**), and final product, butylidenechromium (**2c**). The elements are coded on a gray scale according to H (white) < O < C < Cr (dark gray), and only the oxygen atoms bridging to Cr are shown from the silica cluster. Activation energies in kJ/mol.

the incoming ethylene, and to the alkyl-substituted carbon, representing the growing polymer chain. This reaction may conceivably proceed either in a single step or according to a two-step mechanism involving a hydridochromium intermediate.

The concerted α-H abstraction–H elimination to α-carbon takes place on the triplet energy surface. In the optimized transition state, the reactive hydrogen is coordinated to chromium at a distance of 1.70 Å, with breaking and forming C–H bond lengths 1.63 and 1.44 Å, respectively, cf. **TS[2b-2c]** in Fig. 6 and Table 4. The bond between chromium and C_1 is shortened to 1.86 Å and the geometry about C_1 is approaching planarity, as shown by a dihedral angle, $\angle HC_1CrC_2$, of 174°, both of which indicate formation of double-bond character between C_1 and the metal. The breaking Cr–C_3 bond is stretched to 2.23 Å in the transition state. Energetically, the transition state is found 241 kJ/mol above the chromacyclo(methyl-)butane reactant (**2b**). This is regarded as a prohibitively high barrier.

Alternatively, hydrogen transfer may proceed over two steps, via the formation of a closed-shell chromium(VI) hydride species. Subsequent reductive elimination leads to the product butylidenechromium (**2c**). Such an intermediate was indeed found on the singlet surface, but at an energy only 30 kJ/mol below that of the transition state of the concerted hydrogen transfer reaction. Presumably, the formation of this intermediate is energetically highly demanding, and the details of the reaction have not been determined. The chromium(VI) intermediate displays very short bond lengths both to the hydride and C_1, at 1.56 and 1.72 Å, respectively, and still the chromium–carbon single bond remains essentially intact, at 2.10 Å.

The product, butylidenechromium **2c**, bears the same characteristics with respect to geometry and net charge of chromium as the reactant etylidene complex. The overall energy of the propagation step from **2a** to **2c** is −94 kJ/mol.

TABLE 4

Geometry Parameters for Stationary Points along the Reaction Path of Ethylene Insertion into the Cr=C Double Bond in an Ethylidenechromium Species (2a), with Cycloaddition Product, Chromacyclo(methyl-)butane (2b), the Concerted α-H Transfer Transition State (TS[2b-2c]), and Final Product, Butylidenechromium (2c)

	2a	2b	TS[2b-2c]	2c
$rCrC_1$	—	1.99	1.86	1.82
$rCrC_2$	—	2.34	2.54	3.01
$rCrC_3$	1.82	1.98	2.23	4.26
rC_1C_2	(1.33)[a]	1.55	1.52	1.50
rC_2C_3	—	1.55	1.56	1.54
$rCrH_\alpha$	—	2.61	1.70	—
rC_1H_α	—	1.10	1.63	—
rC_3H_α	—	2.93	1.44	1.10
rCrO	1.79–1.80	1.79–1.80	1.82	1.79–1.80
∠OCrO	112	111	107	113

Note. Units: bond lengths (r) in (Å); angles (∠) in degrees.
[a] Free monomer.

3.3.3. A chroma(IV)cycloalkane site. The facile generation of a chromacyclopentane species (see **3b** in Fig. 4) makes it an interesting starting structure for polymerization. Compared to the analogous dialkyl species that has a tetrahedral configuration about chromium, the acute ∠CCrC angle of 88° and somewhat narrow ∠CrCC angles of 106° in chromacyclopentane leave chromium slightly more exposed. Even so, no coordinative complex was found to form between ethylene and **3b**.

However, with ethylene approaching chromacyclopentane from the side, direct insertion into a Cr–C bond was found feasible. The corresponding transition state is included as **TS[3b-3c]** in Fig. 7. The resulting energy barrier is 119 kJ/mol, i.e., comparable to that of monomer insertion to a dialkylchromium(IV) species. The resemblance holds true also with respect to structural parameters, the main difference being related to the higher strain in the

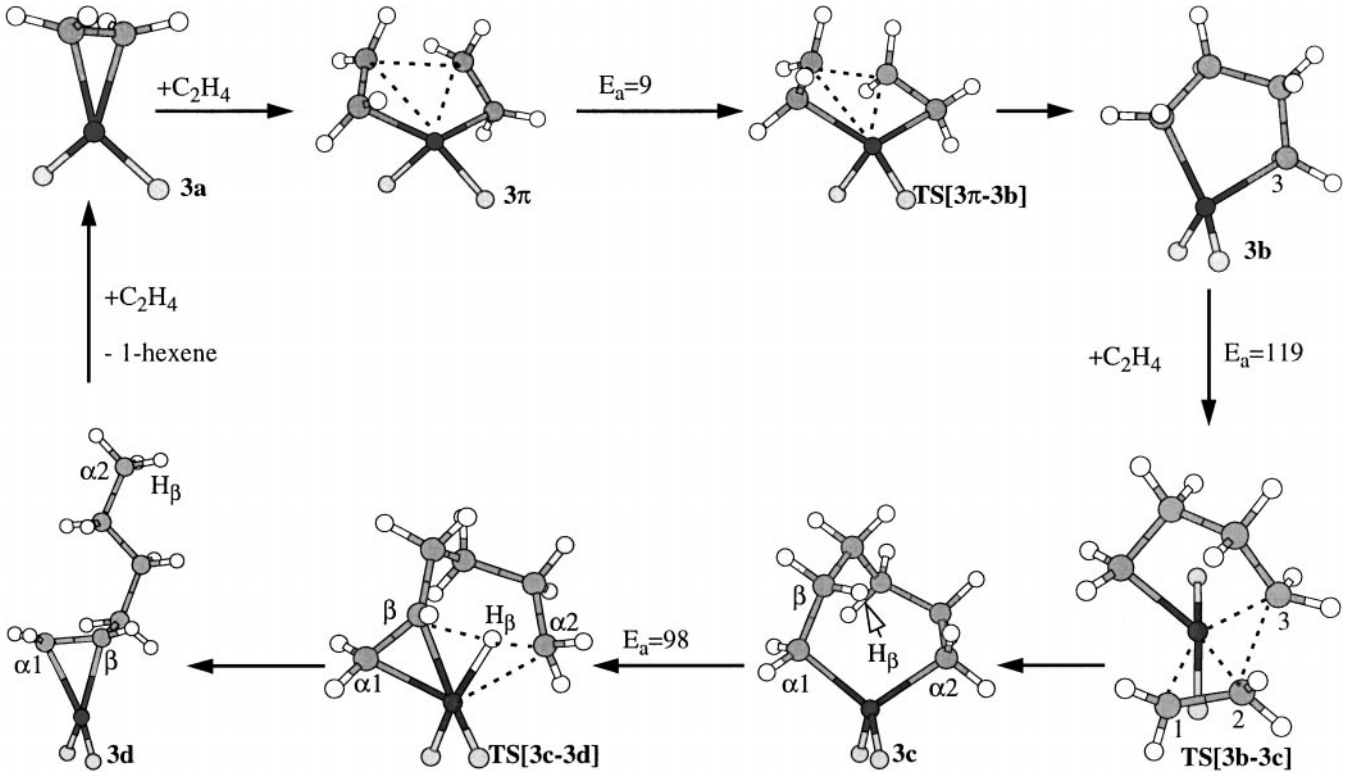

FIG. 7. Stationary points along the reaction path of 1-hexene formation. Structures: **3a**, ^{3}A π-complex; **3π**, double ethylene–Cr π-complex; **TS[3π-3b]**, transition state for cycloaddition; **3b**, chromacyclopentane; **TS[3b-3c]**, transition state for insertion; **3c**, chromacycloheptane; **TS[3c-3d]**, transition state for intramolecular β-H transfer; and **3d**, 1-hexene–Cr π-complex. The elements are coded on a gray scale according to H (white) < O < C < Cr (dark gray), and only the oxygen atoms bridging to Cr are shown from the silica cluster. Activation energies in kJ/mol.

chromacyclopentane ring. This forces the inactive α-carbon closer to chromium, thereby weakening the ethylene coordination in **TS[3b-3c]**, as compared to **TS[1c-1d]** in Fig. 5, cf. Table 3 and Table 5.

The reaction energy of the insertion step to give **3c** is −94 kJ/mol, demonstrating comparable amounts of strain in the five-membered chromacyclopentane reactant and the seven-membered chromacycloheptane product. This is consistent with strain energies of the corresponding cyclic hydrocarbons (48). In the chromacycloheptane product, the ∠CCrC angle opens up to 107°, at the expense of the other angles along the perimeter exceeding the tetrahedral angle by as much as 8°.

The energy barrier toward insertion of a second ethylene remains about the same as that for the first insertion, at 122 kJ/mol. Despite the larger ring, the strain is actually larger in the chromacyclononane product than in the reactant **3c** and the reaction energy decreases to −79 kJ/mol. This is in line with the known ring-strain in the corresponding cycloalkanes (48).

Several studies report the formation of 1-alkenes in the early stages of catalysis, and it is therefore of interest to consider how this finding may be reconciled with mechanisms for polymerization. Starting from a chromacycloalkane intermediate, rearrangement to a coordinated α-olefin may be achieved through intramolecular β-H transfer to the α-carbon at the far end of the carbon chain ($C_{\alpha 2}$, cf. Fig. 7). The corresponding transition state was optimized both for the case of a chromacyclopentane (**3b**) and a chromacycloheptane (**3c**) reactant.

TABLE 5

Geometry Parameters for Stationary Points along the Reaction Path of Ethylene Insertion into a Cr–C Bond in a Chromacyclopentane Species (3b), with Transition State (TS[3b-3c]), and Product, Chromacycloheptane (3c)

	3b	TS[3b-3c]	3c
rCrC$_1$	—	2.19	2.02
rCrC$_2$	—	2.36	2.89
rCrC$_3$	2.02	2.21	—
rCrC$_{\alpha 2}$	2.02	2.07	2.00
rC$_1$C$_2$	(1.33)[a]	1.43	1.53
rC$_2$C$_3$	—	1.99	1.55
rCrO	1.79	1.85–1.86	1.79
∠OCrO	112	95	111

Note. Units: bond lengths (r) in (Å); angles (∠) in degrees.
[a] Free monomer.

TABLE 6

Geometry Parameters for the Reactants and Transition States for Intramolecular β-Hydrogen Transfer in Chromacyclopentane, 3b, and TS[3b- 1-butene], and in Chromacycloheptane, 3c, and TS[3c-3d], Respectively

	3b	TS[3b- 1-butene]	3c	TS[3c-3d]
$r\mathrm{CrH}_\beta$	3.18	1.64	2.90	1.67
$r\mathrm{C}_\beta\mathrm{H}_\beta$	1.10	1.69	1.10	1.55
$r\mathrm{C}_{\alpha 2}\mathrm{H}_\beta$	2.75	1.45	2.88	1.37
$r\mathrm{C}_{\alpha 1}\mathrm{C}_\beta$	1.53	1.43	1.53	1.45
$r\mathrm{CrC}_\beta$	2.85	2.15	2.89	2.18
$r\mathrm{CrC}_{\alpha 1}$	2.02	2.08	2.02	2.02
$r\mathrm{CrC}_{\alpha 2}$	2.02	2.17	2.00	2.21
rCrO	1.79	1.82–1.84	1.79	1.83
$\angle$OCrO	112	104	111	104

Note. Units: bond lengths (r) in Å; angles ($\angle$) in degrees.

A double bond develops between the active β-carbon and the neighboring α-carbon ($\mathrm{C}_{\alpha 1}$), as hydrogen transfer proceeds. This double-bond character facilitates donation of a π-electron to the metal and takes the β-carbon closer to chromium. Consequently, the transition state displays an $(n-1)$ pseudoring structure of the hydrocarbon, where only $\mathrm{C}_{\alpha 1}$ is left out (see Fig. 7 for notation). In the case of a chromacyclopentane reactant, the pseudo ring takes the form of a strained four ring, with an average bond angle of 90° along the carbon backbone. The transition state starting from a chromacycloheptane reactant is characterized by a less strained six-membered pseudo ring, showing an average bond angle of 114°, cf. **TS[3c-3d]** in Fig. 7. The corresponding energy barriers to β-hydrogen transfer are 192 and 98 kJ/mol in the two cases, respectively. The difference in barrier heights matches well the difference in strain energy between cyclobutane and cyclohexane, which is known to be 110 kJ/mol (48).

A closer examination reveals that in the smaller pseudo ring, the ability to maintain significant amounts of $\mathrm{C}{-}\mathrm{H}_\beta$ bonding throughout the transfer process is severely limited, cf. Table 6. Whereas $r\mathrm{C}_\beta\mathrm{H}_\beta + r\mathrm{C}_{\alpha 2}\mathrm{H}_\beta$ equals 2.92 Å for **TS[3c-3d]**, the corresponding number is 3.14 Å in the case of a four-membered pseudo ring. This deficiency is only partly compensated for by coordinating hydrogen closer to chromium.

The reaction energies from chromacycloalkanes to the corresponding triplet-coupled (1-alkene)chromium complexes are computed at 6 and 12 kJ/mol in the case of 1-butene and 1-hexene (**3d** in Fig. 7), respectively. At this point, the alkenes may be released to the gas phase and the divalent chromium site regenerated or, alternatively, an incoming monomer may react with the chromium–alkene complex to form a substituted chromacyclopentane species.

In the latter event, a new polymerization mechanism may be recognized that allows the polymer chain to grow by two monomer units during each cycle. This mechanism involves the formation of a substituted chromacyclopentane species by addition of a monomer to the covalent complex between an α-olefin and chromium. Direct insertion of a second monomer increases the ring size to seven, before a β-H transfer step closes the cycle by regenerating a chromium–olefin complex.

Decoordination of the olefin from the chromium complex may be expected to compete with the generation of a chromacyclopentane derivative only for short 1-alkenes and at low monomer concentrations. The high barrier to β-H transfer within a chromacyclopentane implies that 1-butene will not be formed at all. On the other hand, in the case of a chromacycloheptane reactant species, the corresponding barrier is comparable and even lower than the barrier to direct insertion of a monomer to the ring. This suggests that 1-hexene may be expected to form quite readily in the early stages of catalysis.

3.3.4. Monoalkylchromium(III) site. For completeness, and despite the unresolved question of how a chromium monoalkyl site may be formed initially, we have modelled ethylene insertion to tricoordinate chromium–ethyl species, included as **4a** in Fig. 8. This part of the study follows the Cossee–Arlman mechanism for the propagation step (49), in line with recent studies of homogeneous chromium(III) catalysts for ethylene polymerization (50).

The reactant **4a** displays C_s symmetry, with the ethyl ligand oriented perpendicular to the OCrO plane. In the $^4A''$ ground state, chromium carries three unpaired d electrons and a net charge of 1.31e. Compared to the naked, reduced cluster, the higher positive charge of **4a** leads to slightly contracted chromium–oxygen bonds and a somewhat narrower $\angle$OCrO bond angle. The chromium–carbon

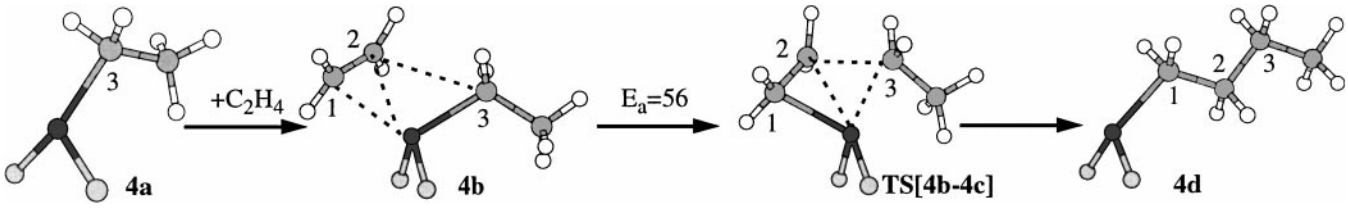

FIG. 8. Stationary points along the reaction path of insertion of ethylene into a monoalkyl chromium structure. Structure: **4a**, ethylchromium; **4b**, π-complex; **TS[4b-4c]**, transition state; **4c**, butylchromium. The elements are coded on a gray scale according to H (white) < O < C < Cr (dark gray), and only the oxygen atoms bridging to Cr are shown from the silica cluster. Activation energy in kJ/mol.

TABLE 7

Geometry Parameters of Stationary Points along the Reaction Path of Ethylene Insertion into the Cr–Ethyl Bond in an Ethylchromium Species (4a) with π-Complex (4b), Transition State (TS[4b-4c]), and Product, Butylchromium (4c)

	4a	4b	TS[4b-4c]	4c
$rCrC_1$	—	2.37	2.05	2.01
$rCrC_2$	—	2.57	2.32	3.03
$rCrC_3$	2.01	2.03	2.19	4.42
rC_1C_2	(1.33)[a]	1.36	1.43	1.52
rC_2C_3	—	3.07	2.09	1.54
$rCrO$	1.81	1.82–1.83	1.84–1.85	1.80
$\angle OCrO$	112	105	104	112

Note. Units: bond lengths (r) in Å, angles ($\angle$) in degrees.
[a] Free monomer.

bond is 2.01 Å, and no important agostic interactions are present.

Ethylene coordinates without activation to the chromium–ethyl complex, forming a π-donation bond at chromium–carbon distances of 2.37 and 2.57 Å, respectively (see **4b** in Fig. 8 and Table 7). The ethylene carbon–carbon bond is barely stretched at all, whereas the net charge on chromium decreases, corresponding to additional 0.07 electrons. Ethylene is bound to the metal by a modest 35 kJ/mol.

The transition state along the path of insertion of ethylene into the chromium–ethyl bond has been determined, c.f. **TS[4b-4c]** in Fig. 8. It has a four-center ring structure consisting of ethylene, chromium, and the α-carbon of the ethyl moiety, consistent with Cossee's proposal for Ziegler–Natta catalysts (51). The present TS is located somewhat late as judged from the lengths of the forming and breaking chromium–carbon bonds, at 2.05 and 2.19 Å, respectively. The central bond of the ethylene moiety has lengthened by 8 pm, to 1.43 Å, and the forming carbon–carbon bond is 2.09 Å. The only notable difference between the parameters listed here and those reported in Ref. (50) is for the forming chromium–carbon single bond, which is reported 5 pm longer in (50) than that found here.

In contrast to what is found for many other polymerization catalysts, the net charge of chromium actually increases slightly toward the transition state, caused by a decline in 4*s* and 4*p* occupation, which outweighs the increase in 3*d* population. The energy barrier to ethylene insertion is computed at 56 kJ/mol relative to the π-complex, **4b**. This is higher than that for any of the homogeneous Cr(III) catalysts considered earlier (50) and probably reflects the less flexible arrangement of ligands as well as the lack of a net positive charge in the present case.

The product, a chromium–butyl species (**4d**), is very similar to the reactant complex as far as geometrical parameters about chromium is concerned. Even this more flexible alkyl is unable to form secondary bonds to the metal. The overall insertion energy is −99 kJ/mol.

3.4. Cluster Size Dependency

Calculations presented hitherto resulted in high activation energies for the following fundamentally different reaction steps: (i) direct insertion of ethylene into a Cr(IV)–alkyl bond, (ii) intramolecular β-H transfer in a chromacycloalkane species, and (iii) intramolecular α-H transfer in a dialkylchromium species. It is of interest to see whether these barriers may be significantly lowered by modifying the model of the site. While retaining a picture of chromium as bonded through two oxygen bridges to silica, the importance of the $\angle OCrO$ angle is examined by remodelling reactions (i–iii) by means of all three cluster models shown in Fig. 3, defined by $n_{Si} = 1$, 2, and 3. This allows $\angle OCrO$ to vary from 85° to 135°, thereby substantially changing the space available to the organic ligands during reaction. Reactions (i and ii) were considered for the special case of ethylene insertion to chromacyclopentane followed by β-H transfer in chromacycloheptane, whereas the last reaction step was modelled by considering a dimethylchromium species with respect to generation of methylidenechromium. To prevent excessive geometric relaxation in the larger $n_{Si} = 3$ cluster, this structure was partially frozen using geometry parameters optimized for the reduced chroma(II)silasesquioxane cage, cf. Fig. 2.

The energy barriers are presented in Table 8 as computed for reactions (i–iii) proceeding on the three cluster models. For all three reaction steps, the activation energy decreases as the $\angle OCrO$ angle narrows. While the differences in E_a between the two smaller clusters are less than 15 kJ/mol for the two hydrogen-transfer reactions, a large reduction of 46 kJ/mol occurs in the barrier to direct insertion. This is accompanied by a push toward an earlier transition state as evident from forming carbon–carbon bond lengths of 1.95, 1.98, and 2.02 Å, for $n_{Si} = 3$, 2, and 1, respectively. For the remaining reactions, apart from obvious differences in the angles associated with the oxygen ester linkages, the optimized geometry parameters agree well with those

TABLE 8

Activation Energy (kJ/mol) of (i) Insertion of Ethylene into a Cr–C Bond in Chromacyclopentane, (ii) β-H Transfer in Chromacycloheptane, and (iii) α-H Transfer in Dimethylchromium on the $n_{Si} =$ 1, 2, and 3 Cluster Models

Cluster	Insertion	β-H Transfer	α-H Transfer
$n_{Si} = 1$	73	85	154
$n_{Si} = 2$	119	98	165
$n_{Si} = 3$	161	114	181

discussed earlier for the $n_{Si} = 2$ cluster. Hence, the changes in barrier heights seem to reflect the available space about chromium. As the ∠OCrO angle widens, the upper part of the Cr coordination sphere becomes more congested, leading to increased repulsion between the ligands. The sterically most demanding reaction considered, i.e., the direct-insertion step, suffers the largest increase in barrier when going from a four-membered to an eight-membered cyclic cluster.

Summarizing, while the activation energies needed in three key reaction steps are found to be notably lower for the highly strained $n_{Si} = 1$ cluster as compared to the larger clusters, the reduction still falls shorts of what is needed to change any conclusions from what already is discussed for the intermediately sized cluster.

4. DISCUSSION

The calculations have shown that both one and two ethylene molecules may coordinate to the reduced Cr(II) cluster, without activation and with considerable binding energy. Only a very low barrier separates the double π-complex from forming a chromacyclopentane structure. Rearrangement of the monoethylene complex to either ethylidenechromium or ethenylhydridochromium, on the other hand, is much less favorable for thermodynamical reasons. Hence, it appears likely that chromacyclopentane is the dominating initial species at the mononuclear Cr(II)-A site.

Several studies report the formation of 1-alkenes in the early stages of Cr-catalyzed polymerization. Jolly and co-workers (27) recently reported that homogeneous chromium-based catalysts may show high selectivity with respect to trimerization of ethylene to 1-hexene. They proposed a mechanism involving chromacyclic intermediates, some of which has been isolated and structurally characterized. Ruddick and Badyal (26) studied the desorbing species on a prereduced Phillips catalyst using mass spectrometry and concluded that only 1-hexene was formed. The formation of 1-hexene ceases as the catalysis goes on, indicating a change in the occupation of these sites to polymerization. Hence, a site that is active for 1-hexene formation might also turn out to be active with respect to polymerization. These findings are compatible with the activity data obtained here for a chromacycloalkane site. In the chromacyclopentane species, the activation energy for intramolecular β-H transfer to produce 1-butene is 100 kJ/mol higher than the barrier toward insertion of ethylene. On the other hand, in chromacycloheptane, β-H transfer is relatively more favorable ($E_a = 98$ kJ/mol), and formation of 1-hexene should compete with chain propagation. As the polymeric chain grows, decoordination of a 1-alkene followed by restarting of the cycle shown in Fig. 7 becomes much less likely than reaction with an incoming monomer, in agreement with the decline in 1-hexene formation as the catalysis goes on.

Even though the *relative* activation energies based on a metallacyclic mechanism are in agreement with the observed early trimerization, an insertion barrier close to 120 kJ/mol is too high to sustain polymerization. Using the dialkylchromium site as a model for a very long chromacycloalkane reactant, this is in line with the lack of activity recently reported by Amor Nait Ajjou *et al.* (22) for a dialkylchromium species anchored to silica through two ester linkages. While these researchers started out from tetraalkylchromium, it is possible that impregnation by chromium oxide may lead to a different geometry of the chromium–substrate coordination, possibly acting to lower the barrier to monomer insertion. Indeed, if the ∠OCrO angle is narrowed, from 116° to 86°, the activation energy for insertion into the Cr–C bond in a chromacyclopentane structure drops from 119 to 73 kJ/mol. Still, the highly endothermic energy computed for the anchoring reaction to produce such a highly strained surface chromium site suggests that this is not a likely process.

The chromacyclopentane species may conceivably rearrange to other structures, which in turn may act as starting points for polymerization. Insertion to an alkyl(allyl)-chromium species occurs with an activation energy in excess of 80 kJ/mol. The kinetics of this reaction is further hampered by the lack of initial coordination of ethylene, a feature that is common for all the tetrahedral chromium(IV) species considered here. The loss of entropy probably adds some 40–50 kJ/mol to the free energy of activation, reflecting the lower probability of a reactive bimolecular collision as opposed to a unimolecular rearrangement.

Returning to Amor Nait Ajjou *et al.*'s (22) line of experiments, they obtained a working catalyst through thermal transformation of dialkylchromium species, accompanied by liberation of an alkane. The stoichiometry of this conversion is consistent with a carbene starting structure. This conclusion is corroborated by Kantcheva *et al.* (21), based on analyses of weak absorptions in an *in situ* Fourier-transform infrared spectroscopic study. The propagation step of the carbene mechanism consists of an initial $2_\pi + 2_\pi$ cycloaddition reaction followed by intramolecular α-hydrogen transfer. Our results for the cycloaddition step agree with findings for a moderately active Ti-based metathesis catalyst, for which the cycloaddition was reported to proceed without barrier (52). The energies required for the hydrogen-transfer step in the tetrahedral high-spin coupled d^2 chromacyclo(methyl-)butane structure (**2b**) are prohibitively high, whether a concerted or a two-step mechanism is considered. Hence, the present cluster model cannot account for regeneration of a carbene species. Since the carbene mechanism for polymerization implies scrambling of hydrogen atoms, this finding is in agreement with McDaniel

and Cantor's conclusion that hydrogen scrambling does not occur during propagation (53).

On the other hand, Amor Nait Ajjou *et al.* obtained evidence in support of an intermolecular α-H elimination mechanism for the preparation of alkylidenechromium from silica-supported dialkylchromium species (24). Magnetic susceptibility measurements support the present assignment of triplet spin states for both the dialkylchromium and alkylidenechromium species. When modelling this reaction in the case of a dimethyl starting structure, the activation energies obtained for α-H transfer are too high to explain the observed transformation at 60–80°C. Following Amor Nait Ajjou *et al.*'s suggestion that coordinating oxygen atoms from nearby siloxane bridges might aid the reaction, coordination of a water molecule was attempted. Whereas the dimethylchromium cluster was unable to bind the water molecule, the product methylidenechromium cluster was stabilized by 52 kJ/mol through a favorable interaction with the water ligand. This aids the overall thermochemistry of the formation of a carbenechromium structure, but coordination of water occurs too late to affect the activation energy. This leaves us with a discrepancy toward Amor Nait Ajjou *et al.*'s findings, suggesting that the generation of carbenechromium species may take place only on surface sites that differ in a qualitative manner from the presently studied disiloxanochromium cluster.

The disiloxanochromium site examined in this work has a strong preference toward the formation of two chromium–carbon single bonds and a tetrahedral coordination about the metal. In such a state, the affinity for additional ligands is low, and in contrast to what is postulated in the Cossee mechanism, a precursor ethylene–chromium complex is not formed. The stability of the tetrahedral arrangement of a disiloxanochromium(IV) species is also reflected in a very high activation energy of the α-hydrogen-transfer reaction in a chromacyclobutane structure. The computed energy barrier of 240 kJ/mol completely rules out the carbene mechanism on the presently studied site. The only reaction mechanism that seems viable on this site is the original Cossee mechanism, involving a three-coordinated monoalkylchromium(III). In this case, a proper precursor is formed without activation, and subsequent insertion to the Cr−alkyl bond is rather facile, with an activation energy of 56 kJ/mol. This value may be compared to activation energies between 25 and 43 kJ/mol computed for the insertion step in homogeneous Cr(III) model systems (50). However, the answer to how the initiation process may proceed to prepare the required monoalkyl- or monohydridochromium starting structure remains elusive. An interesting suggestion (30) in this respect is the formation of a hydrocarbon bridge connecting two neighboring Cr(II)-A sites. In this case, a single ethylene constitutes the starting polymer chain and insertion occurs to either of the two mononuclear Cr(III) atoms. However, especially at low loadings of chromium, such sites are probably rare.

The present findings may be compared to the observed activity toward polymerization of a related model compound. Feher and Blanski (41) synthesized a chromasilasesquioxane, featuring a monochromate moiety bonded through two oxygen atoms to silicon. This molecule displays moderate polymerization activity only after addition of trialkylaluminium. Assuming that ethylene acts to reduce the chromate to a divalent chromium site, the lack of activity without a cocatalyst agrees with the high activation energies obtained here when the starting point is ethylene in contact with a divalent chromium site. Furthermore, the cocatalyst is thought to alkylate the metal, and possibly also to ionize it (54). The process of alkylation is analogous to providing the chromium atom with a hydrido ligand, and we have shown that in this case the insertion reaction proceeds readily and according to the Cossee mechanism. Analogous to an alkylating and ionizing cocatalyst, one may expect a stronger coordination of ethylene if the surface chromium site is supplied with a proton rather than a hydrogen atom (16–18, 55).

Finally, the data presented here suggest that high activity of the Cr(II)-A site presupposes direct participation of the substrate, as opposed to simply binding chromium via two inert oxygen linkages. This participation may occur during the initiation phase, by providing the metal with a starting polymer chain in the form of a hydrogen atom or a proton. Alternatively, surface oxygen atoms, either as silanol groups, exposed siloxane–oxygens, or oxygen atoms linking chromium to the surface, may take an active part in the transfer of α-H, to make the carbene mechanism viable. These possibilities will be examined in future work.

5. CONCLUSIONS

A disiloxanochromium(II) site is shown to coordinate 2 equiv of ethylene, thereby forming a chromacyclopentane structure. An activation energy of about 120 kJ/mol is required to extend the cycle through monomer insertion, with only weak dependency on the ring size. The relative height of the energy barriers with respect to β-hydrogen termination and monomer insertion is in agreement with the observed production of 1-hexene during early stages of polymerization. Since the explanation to a large extent hinges upon the relative amounts of strain in the various cyclic species that appear, these findings are rather stable with respect to changes in the electronic structure of chromium.

Less facile reactions between ethylene and the reduced disiloxanochromium site may give rise to species that are functionally equivalent to dialkylchromium or alkylidenechromium species, featuring chromium in oxidation state IV. The dialkylchromium site provides a path for

chain propagation that is rather similar to the one for a chromacycloalkane site, without the ability to explain the prevalence of 1-hexene. The very high activation energy required for α-hydrogen transfer in a chromacyclobutane structure rules out the carbene mechanism for polymerization for a fully relaxed Cr(II)-A site that maintains two covalent bonds to the silica surface.

For the present model of a disiloxanochromium site, only a three-coordinate monoalkylchromium species is found to support chain propagation with a reaction barrier compatible with catalytic activity, computed at 56 kJ/mol relative to the ethylene–chromium precursor complex. In this case, the insertion reaction follows the original Cossee mechanism, with no important contributions from agostic interactions. However, the issue of how the starting structure may be generated remains unresolved.

The low affinity for ethylene suggests that the presently applied models more closely reflect the properties of Cr–silasesquioxane compounds or, indeed, the majority of Cr atoms at the silica surface, rather than those of the catalytically active sites on Phillips catalysts. These findings point to a more active role for the silica substrate than customarily has been anticipated, possibly in connection with structurally strained coordination sites.

ACKNOWLEDGMENTS

This research was financially supported by The Norwegian Academy of Science and Letters together with Statoil (VISTA) as well as the Research Council of Norway. Access to supercomputer resources was granted by the Research Council of Norway (Programme for Supercomputing). Useful discussions with Dr. Ole Swang during early stages of this work are acknowledged.

REFERENCES

1. McDaniel, M. P., *Adv. Catal.* **33**, 47 (1985).
2. Weckhuysen, B. M., and Schoonheydt, R. A., *Catal. Today* **51**, 215 (1999).
3. McDaniel, M. P., *Ind. Eng. Chem. Res.* **27**, 1559 (1988).
4. Hlatky, G. G., *Chem. Rev.* **100**, 1347 (2000).
5. Theopold, K. H., *Eur. J. Inorg. Chem*. 15 (1998).
6. Thüne, P. C., Verhagen, C. P. J., van den Boer, M. J. G., and Niemantsverdriet, J. W., *J. Phys. Chem. B* **101**(42), 8559 (1997).
7. Weckhuysen, B. M., Wachs, I. E., and Schoonheydt, R. A., *Chem. Rev.* **96**, 3327 (1996).
8. Baker, L. M., and Carrick, W. L., *J. Org. Chem*. **33**, 616 (1968).
9. Krauss, V. H. L., and Stach, H., *Z. Anorg. Allg. Chem*. **366**, 280 (1969).
10. Merryfield, R., McDaniel, M. P., and Parks, G., *J. Catal.* **77**, 348 (1982).
11. Fubini, B., Ghiotti, G., Stradella, L., Garrone, E., and Morterra, C., *J. Catal.* **66**, 200 (1980).
12. Ghiotti, G., Garrone, E., and Zecchina, A., *J. Mol. Catal.* **46**, 61 (1988).
13. Kim, C. S., and Woo, S. I., *J. Mol. Catal.* **73**, 249 (1992).
14. Krauss, H.-L., *J. Mol. Catal.* **46**, 97 (1988).
15. Zecchina, A., Spoto, G., Ghiotti, G., and Garrone, E., *J. Mol. Catal.* **86**, 423 (1994).
16. Rebenstorf, B., *Z. anorg. allg. Chem*. **571**, 148 (1989).
17. Groeneveld, C., Wittgen, P. P. M. M., Swinnen, H. P. M., Wernsen, A., and Schuit, G. C. A., *J. Catal.* **83**, 346 (1983).
18. Joswiak, W. K., Dalla Lana, I. G., and Fiederow, R., *J. Catal.* **121**, 183 (1990).
19. McDaniel, M. P., and Welch, M. B., *J. Catal.* **82**, 98 (1983).
20. Zielinski, P., and Dalla Lana, I. G., *J. Catal.* **137**, 368 (1992).
21. Kantcheva, M., Dalla Lana, I. G., and Szymura, J. A., *J. Catal.* **154**, 329 (1995).
22. Amor Nait Ajjou, J., and Scott, S. L., *Organometallics* **16**, 86 (1997).
23. Amor Nait Ajjou, J., Scott, S. L., and Paquet, V., *J. Am. Chem. Soc.* **120**, 415 (1998).
24. Amor Nait Ajjou, J., Rice, G. L., and Scott, S. L., *J. Am. Chem. Soc.* **120**, 13436 (1998).
25. Krauss, H.-L., and Hums, E., *Z. Naturforsch*. **34b**, 1628 (1979).
26. Ruddick, V. J., and Badyal, J. P. S., *J. Phys. Chem. B* **102**, 2991 (1998).
27. Emrich, R., Heinemann, O., Jolly, P. W., Krüger, C., and Verhovnik, G. P. J., *Organometallics* **16**, 1511 (1997).
28. Espelid, Ø., and Børve, K. J., *in* "Book of Abstracts," C29. WATOC, Royal Soc. Chem., London, Aug. 1999.
29. Spoto, G., Bordiga, S., Garrone, E., Ghiotti, G., and Zecchina, A., *J. Mol. Catal.* **74**, 175 (1992).
30. Rebenstorf, B., and Larsson, R., *J. Mol. Catal.* **11**, 247 (1981).
31. Zecchina, A., Garrone, E., Ghiotti, G., Morterra, C., and Borello, E., *J. Phys. Chem*. **79**, 966 (1975).
32. Baerends, E. J., Bérces, A., Bo, C., Boerrigter, P. M., Cavallo, L., Deng, L., Dickson, R. M., Ellis, D. E., Fan, L., Fischer, T. H., Guerra, C. F., van Gisbergen, S. J. A., Groeneveld, J. A., Gritsenko, O. V., Harris, F. E., van den Hoek, P., Jacobsen, H., van Kessel, G., Kootstra, F., van Lenthe, E., Osinga, V. P., Philipsen P. H. T., Post, D., Pye, C. C., Revenek, W., Ros, P., Schipper, P. R. T., Schreckenbach, G., Snijders, J. G., Sola, M., Swerhone, D., te Velde, G., Vernooijs, P., Versluis, L., Visser, O., van Wezenbeek, E., Wiesenekker, G., Wolff, S. K., Woo, T. K., and Ziegler, T., "ADF 2.3.0 Parallell Computer Code", 1997.
33. Guerra, C. F., Snijders, J. G., te Velde, G., and Baerends, E. J., *Theor. Chem. Acc.* **99**, 391 (1998).
34. Vosko, S. H., Wilk, L., and Nusair, M., *Can. J. Phys.* **58**, 1200 (1980).
35. Perdew, J. P., *Phys, Rev. B* **33**, 8822 (1986).
36. Becke, A. D., *Phys. Rev. A* **38**, 3098 (1988).
37. Frisch, M. J., Trucks, G. W., Schlegel, H. B., Gill, P. M. W., Johnson, B. G., Robb, M. A., Cheeseman, J. R., Keith, T., Petersson, G. A., Montgomery, J. A., Raghavachari, K., Al-Laham, M. A., Zakrzewski, V. G., Ortiz, J. V., Foresman, J. B., Peng, C. Y., Ayala, P. Y., Chen, W., Wong, M. W., Andres, J. L., Replogle, E. S., Gomperts, R., Martin, R. L., Fox, D. J., Binkley, J. S., Defrees, D. J., Baker, J., Steward, J. P., Head-Cordon, M., Gonzalez, C., and Pople, J. A., "Gaussian 94 Computer code." Gaussian Inc., Pittsburgh, PA, 1995.
38. Jensen, V. R., and Børve, K. J., *J. Comput. Chem*. **19**, 947 (1998).
39. Flanigen, E. M., Bennet, J. M., Grose, R. W., Cohen, J. P., Patton, R. L., Kirchner, R. M., and Smith, J. V., *Nature* **271**, 512 (1978).
40. Sauer, J., *Chem. Rev.* **89**, 199 (1989).
41. Feher, F. J., and Blanski, R. L., *J. Chem. Soc., Chem. Commun.* 1614 (1990).
42. Espelid, Ø., Børve, K. J., and Jensen, V. R., *J. Phys. Chem. A* **102**, 10414 (1998).
43. Weckhuysen, B. M., and Wachs, I. E., *J. Chem. Soc., Faraday Trans.* **92**, 1969 (1996).
44. Weckhuysen, B. M., De Ridder, L. M., and Schoonheydt, R. A., *J. Phys. Chem*. **97**, 4756 (1993).
45. Maitland, J., *in* "Organic Chemistry," Chap. 6.1, pp. 196–197. Norton, New York, 1999.
46. Hérisson, J.-L., and Chauvin, Y., *Makromol. Chem*. **141**, 161 (1970).

47. Soufflet, J.-P., Commereuc, D., and Chauvin, Y., *Acad. Sci. Paris* **276**, 169 (1973).
48. Isaacs, N. S., *in* "Physical Organic Chemistry," Chap. 8, p. 283. Longman Scientific & Technical, New York, 1995.
49. Cossee, P., *Tetrahedron Lett.* **17**, 12 (1960).
50. Jensen, V. R., Angermund, K., Jolly, P. W., and Børve, K. J., *Organometallics* **19**, 403 (2000).
51. Cossee, P., *J. Catal.* **3**, 80 (1964).
52. Upton, T. H., and Rappé, A. K., *J. Am. Chem. Soc.* **107**, 1206 (1985).
53. McDaniel, M. P., and Cantor, D. M., *J. Polym. Sci. Polym. Chem. Ed.* **21**, 1217 (1983).
54. Mülhaupt, R., *in* "Ziegler Catalysts," (G. Fink, R. Mülhaupt, and H. H. Brintzinger, Eds.), Chap. 3. Springer Verlag, Berlin, 1995.
55. Nishimura, M., and Thomas, J. M., *Catal. Lett.* **21**, 149 (1993).